SM Online
Scientific Resources
SM Journal of Biomedical Engineering

Research Article

Non-Linear Energy Harvesting Due to Large Amplitude Vibrations of Coupled Impacting Piezoelectric Cantilever Beams

Peyman Firoozy*

Department of Mechanical Engineering, Tarbiat Modares University, Iran

Article Information

Received date: Dec 10, 2017
Accepted date: Jan 18, 2018
Published date: Jan 22, 2018

***Corresponding author**

Peyman Firoozy, Department of Mechanical Engineering, Tarbiat Modares University, Tehran, Iran, Email: p.firoozy@modares.ac.ir

Keywords Energy harvesting; Unimorph piezoelectric; Cantilever beam; Large amplitude vibrations; Coupled impacting system

Abstract

This paper investigates the mechanical behaviour of a system consisting of two coupled impacting unimorph piezoelectric cantilever beams, where the whole system is subjected to a harmonic base excitation, for energy harvesting. The system is modelled as in-extensional beams with Euler-Bernoulli beam theory. The curvature term is assumed to be nonlinear due to large amplitude vibrations. The governing equations of motion are derived using the Euler-Lagrange equations. The reduced-order model equations (ROMs) are obtained based on the Galerkin method. A parametric study is performed to reveal the influence of different parameters such as clearance between beams, coupling spring constant, damping ratio and external resistance load on the scavenged power from the nonlinear energy harvester. It is shown that the power generated by the coupled impact system due to nonlinear vibrations is sensitive to the thickness ratio of the beams and piezoelectric layers, and the clearance between the beams. In addition, the effect of the external resistance load on the average power is discussed for three types of systems: 1) a system which consists of two beams without impact, 2) a system which consists of two beams with impact, and 3) a system which consists of a single beam. The optimum value of the resistance load is obtained for each system, and it is shown that higher power is harvested by a system consisting of two beams with impact than other two systems.

Introduction

In last few years, the requirement for harvesting energy from ambient vibrations of natural environments, such as air flows and human motions, which are available everywhere and all the time, has gained impetus among many researchers. One main purpose of these researches is to power small electrical components such as batteries and capacitors, with no need of replacement, especially at less accessible locations. Researchers are working on alternative energy sources such as solar, acoustics, thermal, and vibrations [1,2]. Among these alternative sources, environmental vibration energy harvesting has become a prominent research endeavour, owning to its potential and technical challenge, and because of its abundance[3, 4]. The ambient mechanical vibration energies can be converted to useful electrical energy by using electromagnetic, electrostatic, piezoelectric [2,5-8]and magnetostrictive [9,10] methods. Among these transduction methods, piezoelectric energy harvesting from cantilever beams; owing to its easy application; has been widely focused in the literature [11-13].The main problems associated with this vibrational energy harvester systems are in their conventional form. The problem is that the harvested power drops significantly when the excitation frequency slightly deviates from the natural frequency of the system. Meantime, broadening bandwidth to adjust vast frequency vibrations usually results in a decrease in the Q-factor. The other problem is the incompetent low frequency energy harvesting. Shifting the resonant frequency to adjust lower vibration frequency usually accompanies a decrease in the Q-factor, and consequently, a drop in the harvested power [12,14]. In order to solve those problems and improve the performance of the energy harvesters, many experiments have been conducted. A way to attain a wideband vibration energy harvesting and keeping high Q-factor simultaneously is introduced, for example, by using non-linear spring [15,16], and bistable spring [17-19]. In addition, there are many researches on adjusting the vibration characteristics of an energy harvester by tuning the excitation frequency. These include added masses [20,21], mechanical preloads [22] and varying the geometrical parameters of the structure [23]. Naguyen et al. [15] fabricated and modelled a wideband MEMS electrostatic energy harvester by utilizing nonlinear spring to broad the frequency range. They experimentally concluded that the vibration energy harvester exhibit a strong softening spring effect. Furthermore, they showed that the vibration energy harvester with softening spring increases the bandwidth and also scavenges more output power than a linear energy harvester. In addition, they have carried out numerical analysis to confirm that the softening springs are reliable for broadening the frequency ranges. Barton et al. [16] investigated a nonlinear electromagnetic energy harvesting device that has a broad resonance response by considering a nonlinear cubic force in boundary conditions. They concluded that the benefit of using a nonlinear energy harvester is the

presence of a super-harmonic resonance at frequencies well below the linear natural frequency. Ferrari et al. [17] designed and tested a nonlinear bistable piezoelectric converter for vibration energy harvesting from environment. Their analysis and simulations showed that utilizing a nonlinear bistable energy harvester enhance performance of the system under wideband excitation frequency with respect to the linear systems. Their experimental tests were performed by measuring both the beam displacement and output voltage under random excitation in different degrees of nonlinearity added to the system. They have concluded that the output voltage at equality of mechanical excitation remarkably improved when the system has become bistable. Panyam et al. [24] studied analytical techniques to predict the oscillatory response characteristics of bi-stable vibratory energy harvesters. They investigated the influence of the three parameters, such as, time constant ratio, electromechanical coupling, and potential shape, on the effective bandwidth. They concluded that the frequency bandwidth can be increased simply by increasing the amplitude of the excitation frequency, also they concluded that the influence of the constant ratio is not considerable on the effective bandwidth. In addition, they concluded that the influence of the electromechanical coupling is significant where increasing the electromechanical coupling results in the narrowing of the effective bandwidth. Jiang et al. [20] investigated the performance of a piezoelectric bimorph in the flexural mode for energy harvesting from ambient vibrations. They analytically concluded that the output power density initially increases, and reaches to a maximum value, and then monotonically decreases with increasing resistance load. Impact is presented and modelled in different ways and for different purposes in vibration energy harvesting systems. Impact with end stop that limits the displacement of the beam where the impact non-linearly broadens the frequency range [25-27]. Soleiman et al. [25] designed a new architecture for wideband vibration-based Micro Power Generators (MPGs). The new system architecture replaces the standard linear oscillator with a piecewise linear oscillator to harvest environmental vibrations. They theoretically and experimentally concluded that the new architecture increases the bandwidth of the MPGs during an up-sweep compared to the traditional MPG. Julin Blystad et al. [26] investigated the effect of the stoppers and power conversion circuitry on the performance of an energy harvesting system subjected to harmonic and wideband excitations. They concluded that frequency sweep with constant excitation amplitude resulted in nonlinear behaviour of the transducer which shows jump phenomena at certain frequencies. In contrast to harmonic excitation, wideband excitations give a considerable output power sensitivity to stopper loss which means that design of energy harvester subjected to the wideband excitation will benefit by minimizing the stopper loss. Many researches were conducted to increase the deformation of piezoelectric material and consequently the output power by utilizing impact associated with piezoelectric transduction in vibration energy harvesters [28-30]. Umeda et al. [28] investigated the fundamental of a generator which transforms the mechanical impact energy to electrical energy by utilizing a piezoelectric material and a steel ball. They concluded that the spectrum of the output voltage is changing by resistance load, and there exists an optimum value for resistance load in which the output voltage reaches to its maximum value. Haroun et al. [31] investigated an electromagnetic energy harvesting based on Free/Impact Motion (FIEH) and Similar Conventional Form (CEH). In FIEH, a permanent magnet mass is permitted to move freely within a certain distance inside a frame which carrying an electrical coil and makes impact with spring and stops. Their simulations and experimental results showed the superior performance of FIEH at low frequency. Vijayan et al. [32] investigated the possibility of similar effects within a non-linear system. A system consisting of two beams with a localized non-linearity induced by an impact was modelled theoretically to explore the effect of frequency up conversion on the power generated from the harvester. They found optimum values of physical and electrical constants such as thickness ratio of the beams, external resistance load and the clearance. Based on the literature, utilizing nonlinear properties of energy harvesting system can significantly affect the average scavenged power over a broad frequency range. It can be found out that there are few researches in the literature that have presented comprehensive investigation on two coupled impacting piezoelectric beams, as an energy harvester, in the presence of geometric nonlinearities. This study attempts to provide a complete dynamical model for an energy harvester system, comprised of two coupled impacting piezoelectric cantilever beams, by considering the geometric nonlinearities of the beams. It is assumed that the beams undergo large amplitude vibrations. The aim of this study is to harvest energy at low excitation frequencies. The effect of different physical parameters such as, clearance between beams, coupling spring constant, thickness ratio of the beams and piezoelectric layers, mechanical damping ratio, and also the effect of the external resistance load for three different types of the systems: 1) a system which consists of two beams without contact, 2) a system which consists of two beams with impact, and 3) a system which consists of a single beam are investigated. This paper reports theoretical and numerical investigations for the considered nonlinear energy harvester.

Methods

Electro mechanical Equations of the coupled impacting beams

For energy harvesting, a system consisting of two nonlinear cantilever beams and an attached unimorph piezoelectric patch for each beam is considered where whole system is excited harmonically through the base. The governing equations of motion are obtained based on the Euler-Bernoulli beam theory and the shear deformations are ignored due to the large length-to-thickness ratio of the beams. The relations between displacement and curvature are supposed to be nonlinear due to the large amplitude vibrations. To include the complete contribution of the piezoelectric patches in the system dynamics, the effect of the mass and the inertia of the piezoelectric layers are considered in the proposed model.

(Figure 1) depicts the considered nonlinear energy harvester that consists of two unimorph piezoelectric cantilever beams. The beams are of length L_b and thickness t_{bi}; and the piezoelectric layers are of length L_{pi} and thickness t_{pi} where i indicates the number of the beams and piezoelectric layers. The width of the piezoelectric layers and the beams are equal $w_{bi} = w_{pi}$. The whole system is subjected to a harmonic base excitation, $z(t) = z_0 \sin(\omega_e t)$, where z_0 and ω_e are excitation and frequency amplitudes, respectively. The transverse and axial displacements are denoted by $v_i(s,t)$ and $u_i(s,t)$, respectively, where s denotes the distance along the neutral axis of the beams. For the sake of simplicity, it is assumed that the beams have a uniform mass distribution. The total kinetic energy of the system is composed

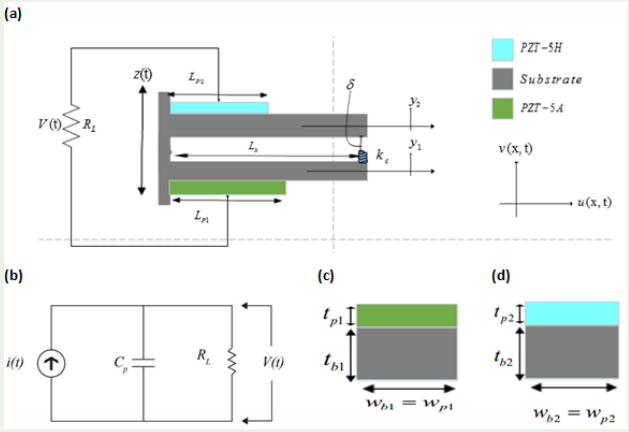

Figure 1: A schematic of a nonlinear energy harvesting system. **(a)** Piezoelectric cantilever beams with unimorph configuration under translational base excitation $z(t)$, **(b)** The corresponding electrical circuit with a dependent current source, **(c)** the cross section of the piezoelectric cantilever beam #1 (thin beam), **(d)** the cross section of the piezoelectric cantilever beam #2 (thick beam).

of the kinetic energies of the cantilever beams, and piezoelectric patches. The kinetic and potential energies of the piezoelectric cantilever beams is defined as [33-35]:

$$T_{(T_i)} = \frac{1}{2}(\rho_{bi}A_{bi})\int_0^{L_b}\left[\frac{1}{4}\left(\frac{\partial}{\partial t}\int_0^s v_i'^2 ds\right)^2 + (\dot{v}_i+\dot{z})^2\right]ds + \frac{1}{2}(\rho_{pi}A_{pi})\int_0^{L_{pi}}\left[\frac{1}{4}\left(\frac{\partial}{\partial t}\int_0^s v_i'^2 ds\right)^2 + (\dot{v}_i+\dot{z})^2\right]ds \quad \text{(eq 1)}$$

where A_{bi} and A_{pi}, ρ_{bi} and ρ_{pi} are cross sectional areas, mass density of the beams, and the piezoelectric layers, respectively and dot denotes the derivative with respect to *t*. The total potential energy of the system is composed of the strain and gravitational energy of the piezoelectric beams, and the potential energy of the coupling spring, and is given by:

$$\begin{aligned} U_{T_i} &= \frac{1}{2}E_{bi}I_{bi}\int_0^{L_b}\left[v_i''^2\left(1+v_i'^2\right)\right]ds + \frac{1}{2}E_{pi}I_{pi}\int_0^{L_{pi}}\left[v_i''^2\left(1+v_i'^2\right)\right]ds \\ &+\rho_{bi}g\int_0^{L_b}\left(v_i(s,t)+z(t)\right)+\rho_{pi}g\int_0^{L_{pi}}\left(v_i(s,t)+z(t)\right) \\ &+\frac{1}{2}k_c\left(v_2(L_b,t)-v_1(L_b,t)-\delta\right)^2 u\left(v_2(L_b,t)-v_1(L_b,t)-\delta\right) \end{aligned} \quad \text{(Eq.2)}$$

where E_{bi} and E_{pi}, I_{bi} and I_{pi}, and U_{spring}, are Young's modulus and the area moment of inertia of the beams and the piezoelectric layers, and the potential energy of the coupling spring which is obtained in the following, respectively. g is the gravitational constant.

In this study, the piezoelectric material is used to convert the mechanical bending strain into the electrical charge. Piezoelectric beams as energy harvesters, are modelled in different shapes and configurations. Depending on the piezoelectric patch configuration, they are categorized as either unimorph or bimorph. In the current study, the considered piezoelectric cantilever beams are in the unimorph configuration.

It is assumed that the continuous electrodes that cover top and bottom of the thick and thin beams, respectively, where the piezoelectric element is located, are perfectly conductive. Therefore, the induced electric field in the piezoelectric layers is supposed to be uniform through the beams. Suppose the piezoelectric element layers are in either unimorph or bimorph configuration. From the previous published papers one may obtain the following electromechanical equation [33-35]:

$$\frac{V(t)}{R_l} + C_p\frac{dV(t)}{dt} = -\sum_{i=1}^{2}\int_0^{L_{pi}}\gamma_{ci}\frac{d}{dt}\left[v_i''\left(1+\frac{1}{2}v_i'^2\right)\right]dx \quad \text{(Eq. 3)}$$

where $C_p = C_{p1} + C_{p2}$.

The reduced-order model

To obtain the reduced-order model of the electromechanical equations of motion,the Galerkin discretization method is utilized, and the transverse displacement of the beams is approximated as [36]:

$$v_i(x,t) = \sum_{j=1}^{n}\varphi_j(x)q_j(t) \quad \text{(eq. 4)}$$

where $\varphi_j(x)$ is the Eigen function of the cantilever beam, as a comparison function, and $q_j(t)$ is the associated time-varying generalized coordinates. By considering one-mode approximation, Eq. [35] reduces to:

$$v_1(x,t) = \varphi_1(x)q_1(t) \quad \text{(eq.5)}$$

$$v_2(x,t) = \varphi_2(x)q_2(t) \quad \text{(eq.6)}$$

where 2 in subscripts of the $\varphi_2(x)$ and $q_2(t)$ in Eq.6 does not indicate the second mode, and these are independent from of $\varphi_1(x)$ and $q_1(t)$, respectively. $\varphi_1(x)$ and $\varphi_2(x)$ can be obtained by solving the eigen value problem of an undamped cantilever beam, and are introduced in the [33-35].

By substituting Eqs.5 and 6 into Eqs. 1, 2 and 3 one may obtain the following reduced order electromechanical equations as:

$$\begin{aligned} &\left(1+\frac{k_1}{k_2}q_1^2\right)\ddot{q}_1 + \omega_{n1}^2 q_1 + 2\xi\omega_{n1}\dot{q}_1 + \frac{k_3}{k_2}q_1^3 + \frac{k_1}{k_2}q_1\dot{q}_1^2 - \frac{\theta_1}{k_2}V(t) - \frac{\theta_2}{k_2}q_1^2V(t) \\ &-\frac{k_c}{k_2}\left(k_7k_8q_2 - k_8^2q_1 - \delta\right)u\left(k_7q_2 - k_8q_1 - \delta\right) + \frac{k_5}{k_2} + \frac{k_6}{k_2}\ddot{z} = 0 \end{aligned} \quad \text{(Eq.7)}$$

$$\begin{aligned} &\left(1+\frac{k_9}{k_{10}}q_2^2\right)\ddot{q}_2 + \omega_{n2}^2 q_2 + 2\xi\omega_{n2}\dot{q}_2 + \frac{k_{11}}{k_{10}}q_2^3 + \frac{k_9}{k_{10}}q_2\dot{q}_2^2 - \frac{\theta_3}{k_{10}}V(t) \\ &-\frac{\theta_4}{k_{10}}q_2^2V(t) - \frac{k_c}{k_{10}}\left(k_7^2q_2 - k_7k_8q_1 - \delta\right)u\left(k_7q_2 - k_8q_1 - \delta\right) + \frac{k_{13}}{k_{10}} + \frac{k_{14}}{k_2}\ddot{z} = 0 \end{aligned} \quad \text{(Eq.8)}$$

where ξ denotes the viscous damping coefficient, and coefficients $k_{i=1..14}$ are defined as follows:

$$\begin{aligned} k_1 &= \rho_{b1}A_{b1}N_4 + \rho_{p1}A_{p1}N_4 \\ k_2 &= \rho_{b1}A_{b1}N_2 + \rho_{p1}A_{p1}N_5 \\ k_3 &= 4\left(N_{13} + N_{15}\right) \\ k_4 &= 2\left(N_{14} + N_{16}\right) \\ k_5 &= \rho_{b1}gN_{17} + \rho_{p1}gN_{18} \\ k_6 &= \rho_{b1}A_{b1}N_7 + \rho_{p1}A_{p1}N_6 \end{aligned}$$

$$k_7 = N_{25}$$
$$k_8 = N_{26}$$
$$k_9 = \rho_{b2}A_{b2}N_7 + \rho_{p2}A_{p2}N_{10}$$
$$k_{10} = \rho_{b2}A_{b2}N_8 + \rho_{p2}A_{p2}N_{11}$$
$$k_{11} = 4\left(N_{19} + N_{21}\right)$$
$$k_{12} = 2\left(N_{20} + N_{22}\right)$$
$$k_{13} = \rho_{b2}gN_{23} + \rho_{p2}gN_{24}$$
$$k_{14} = \rho_{b2}A_{b2}N_9 + \rho_{p2}A_{p2}N_{12} \quad \text{(Eq. 9)}$$

The natural frequency of the beams (i.e. ω_{ni}), can be evaluated by dropping the nonlinear terms and neglecting the mechanical damping ratio and for short circuit conditions (i.e. $R_1 \to 0$), as follows:

$$\ddot{q} + \frac{k_4}{k_2}q = 0 \Rightarrow \omega_{n1} = \sqrt{\frac{k_4}{k_2}} \quad \text{(Eq.10)}$$

$$\ddot{q} + \frac{k_{12}}{k_{10}}q = 0 \Rightarrow \omega_{n2} = \sqrt{\frac{k_{12}}{k_{10}}} \quad \text{(Eq.11)}$$

By substituting Eqs.5, and 6 into Eq.4 and using $\theta_{1..4}$ (see the Appendix) the electrical circuit equation reduces to:

$$C_p\frac{dV(t)}{dt} + \frac{V(t)}{R_l} = -[\theta_1\dot{q}_1 + \theta_2 q_1^2\dot{q}_1 + \theta_3\dot{q}_2 + \theta_4 q_2^2\dot{q}_2 \quad \text{(Eq.12)}$$

The average power that is scavenged between times t_1 and t_2 can be evaluated by:

$$P_{ave} = \frac{1}{t_2 - t_1}\int_{t_1}^{t_2}\frac{V(t)^2}{R_l}dt \quad \text{(Eq.13)}$$

Numerical Results and Discussions

In this section, the numerical results are presented. The numerical simulation results are obtained by using ode 45 in MATLAB software. The numerical simulations are performed for the case study of PZT-5A and PZT-5H, for which physical properties and electrical constants are listed in Table 1.

Figure 2 investigates the influence of the beams length on the impact force of the coupled impacting beams for physical and electrical parameters of the Table 1. The clearance, coupling spring constant, length of the piezoelectric layers #1 and #2 were fixed at δ=15 mm, k=10^3N/m, $L_{P_1} = L_{P_2} = 10mm$, respectively. The excitation frequency is considered to be equal to corresponding primary resonance frequency of the system for each value of the beams length. It is seen that for some range of beams length, the beams do not have contact with each other and impact does not occur in the system, and for other values of the beams length, i.e. $L_b \geq 90mm$ the beams begin to contact with each other and impact happens between them. It can be seen that as the beams length increases the amplitude of the contact force is increased. It is worthy to note that further analysis is carried out by considering $L_b = 300mm$ as the length of the beams.

Figure 3 Depicts the time history of the contact force for different values of the clearance δ, and for external resistance load of $R_L = \Omega 2M$, base acceleration 9.81m/s^2, mechanical damping ratio $\xi = 0.5\%$, Excitation frequency $\omega\_e = 3.08\ Hz$, which is equal to resonance frequency of the thick beam, and the coupling constant of $k = 500\,N/m$, the length of the piezoelectric layers of $L_{P_1} = 100mm$, and $L_{P_2} = 150mm$. Because the purpose of this paper is to study energy harvesting from impacting beams, so, it is important to identify when and for what values of the clearance impact occurs between the beams. According to Eq.2 the contact force occurs when the clearance between beams δ is less than the relative displacement $(y_2 - y_1)$. As it is seen when the clearance is more than δ>470 mm the impact does not occur between the beams and each beam behaves independently. It is seen that for small values of the clearance, the amplitude of the impact force is larger than the large values of the clearances. In addition, it can be seen from the first column of the Figure 3, the system would have chaotic or periodic behaviour when the impact occurs and does not occur in the system, respectively. The results are obtained using the zero initial conditions for the tip displacements and velocities.

Figure 4 illustrates a parametric study on the tip displacement of the beams which was carried out using a sine sweep across a frequency range for the base acceleration, the coupling spring constant, and clearance between beams fixed at $10\,m/s^2$, $k = 400\,N/m$, and δ=10 mm respectively, while the external resistance load is varying simultaneously. A sine sweep in excitation frequency and external resistance load was carried out from 0 to 8 Hz, and 0.1 to 3 MΩ, respectively. It can be observed that the maximum amplitude

Table 1: Geometry and material properties of the studied piezoelectric energy harvester.

Symbol and value	Description
L_b = 100 mm	Length of the beams
w_{b1} = 15 mm	Width of the thin beam
w_{b2} = 20 mm	Width of the thick beam
t_{b1} = 0.5 mm	Thickness of the thin beam
t_{b2} = 0.5 mm	Thickness of the thick beam
t_{p1} = 0.4 mm	Thickness of the PZT-5A
t_{p2} = 0.4 mm	Thickness of the PZT-5H
E_{b1} = 110 GPa	Young's modules of the thin beam
E_{b1} = 105 GPa	Young's modules of the thick beam
E_{p1} = 61 GPa	Young's modules of the PZT-5A
E_{p2} = 60.6 GPa	Young's modules of the PZT-5H
ρ_{b1} = 7320 kg/ m^3	Mass density of the thin beam
L_{pi} = 9000 kg/ m^3	Mass density of the thick beam
ρ_{p1} = 7750 kg/ m^3	Mass density of the PZT-5A
$w_{b_1} = w_{p_1}$ = 7500 kg/ m^3	Mass density of the PZT-5H
$d_{31}^{\ 1} = -171\,pm/V$	PZT-5A constant
$d_{31}^{\ 2} = -274\,pm/V$	PZT-5H constant
$\varepsilon_{33}^S = 13.3\,nF/m$	PZT-5A permittivity
$\varepsilon_{33}^S = 25.55\,nF/m$	PZT-5H permittivity

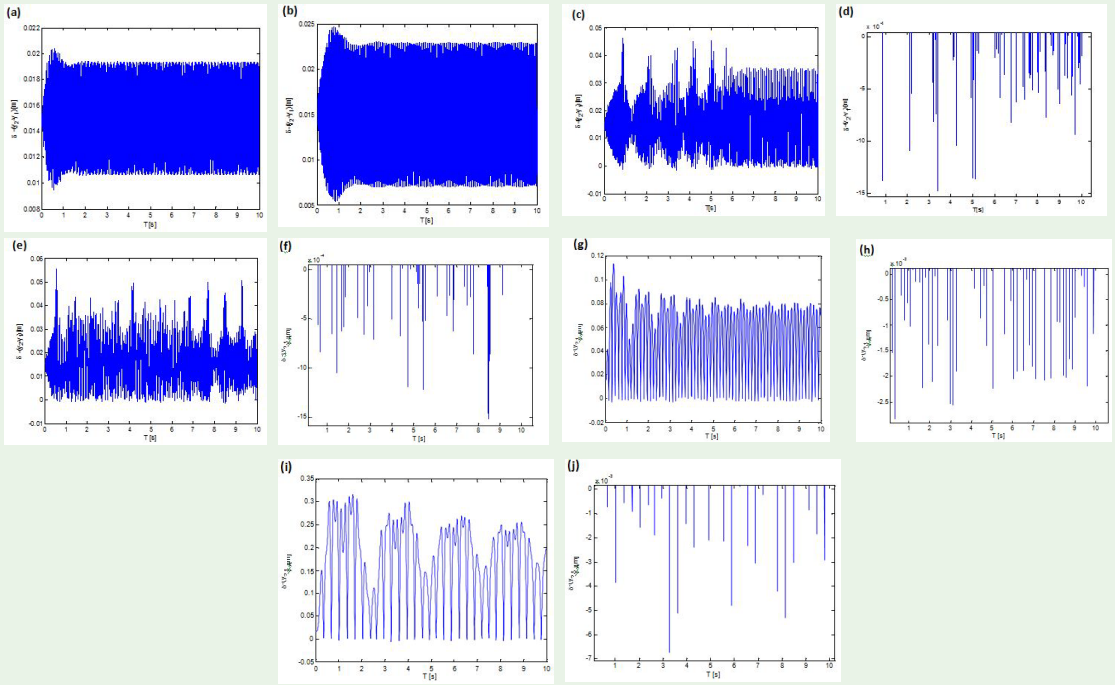

Figure 2: The impact force duration of the coupled impacting beams for different values of the beams length **(a)** L_b= 70mm, **(b)** L_b= 80mm, **(c,d)** L_b= 90mm, **(e,f)** L_b=100mm, **(g,h)** L_b=200mm, **(i,j)** L_b=300mm.

for each beam occurs at the excitation frequency of $\omega_e = 3.01Hz$ which is close to primary resonance frequency of the thick beam. In addition, the value of the external resistance load in which the maximum amplitude of beam #1, and #2 occurs is 2.8 MΩ, and 2.23 MΩ respectively. Since the response of the system is relatively high near the resonance frequency of the thick beam, i.e. $\omega_n = 3.08Hz$, further analysis is carried out for the base excitation of the system at this frequency.

Figure 5 depicts the influence of the clearance on the maximum average output power and the tip displacements of the beams, corresponding to the parameters and loading conditions of Figure 3, and for the coupling constant of $k = 400\,N/m$, while the external resistance load is varying simultaneously. As it can be seen, the maximum power and tip displacements occurs for the small range of the clearances where the impact possibility is high and amplitude of the impact force between the beams is large, as discussed in Figure 3.

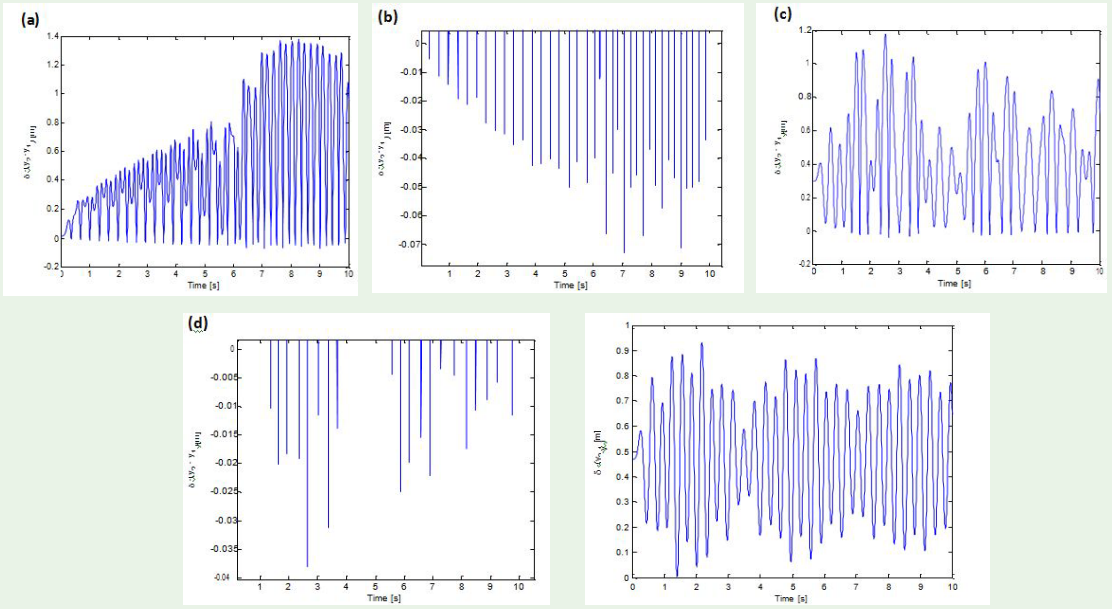

Figure 3: Impact force duration of the coupled impacting beams for three different values of the clearance, **(a,b)** $\delta = 15mm$, **(c,d)** $\delta = 300mm$, **(e)** $\delta = 470mm$.

Citation: Firoozy P. Non-Linear Energy Harvesting Due to Large Amplitude Vibrations of Coupled Impacting Piezoelectric Cantilever Beams. SM J Biomed Eng. 2018; 4(1): 1024s.

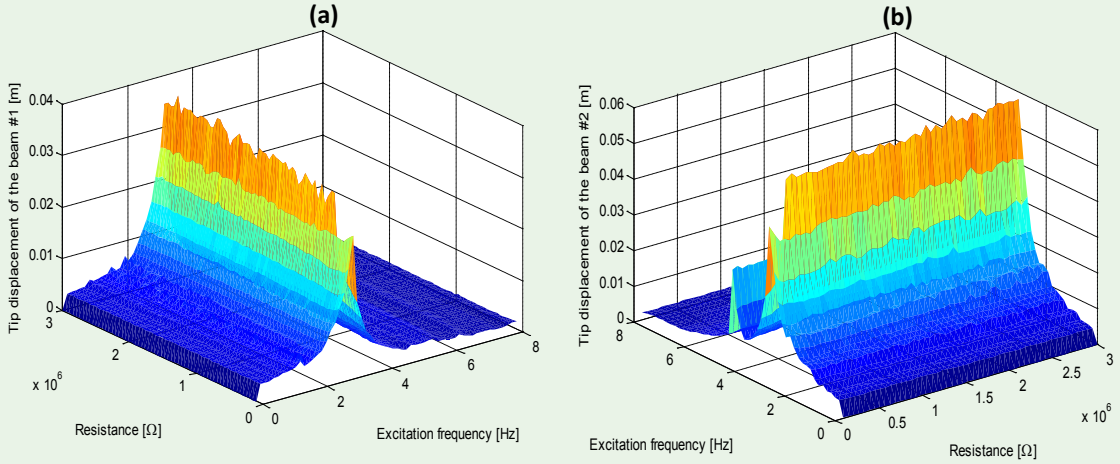

Figure 4: The stepped sine responses of the, **(a)** thin beam (beam #1), **(b)** thick beam (beam #2) with respect to external resistance load, for the base acceleration, the coupling constant, and clearance between beams at, $10\,m/s^2$, $k=400\,N/m$ and $\delta=470mm$, respectively.

As it is seen the maximum average output power produced by large amounts of the clearance (δ>76 mm) is less sensitive to clearance, and the maximum value of the average output power occurs at δ=46mm and $R_L=$ ÌM , and is equal to 20 mW.

Figure 6 depicts the influence of the clearance and coupling constant on the maximum average output power, corresponding to the parameters and loading conditions of Figure 3, and for the external resistance load of $R_L=$ 0Ì8M , and the base acceleration level of $1\,m/s^2$, while they are varying simultaneously. As it is seen the maximum average output power is equal to 35.4 μW and occurs at δ=35 mm and $k_c=240.8\,N/m$. In addition, it can be seen that the produced output power is less sensitive for δ>60 mm and for all values of the coupling constant. Also the influence of the base acceleration can be found by comparing the Figure 4c and Figure 5 where it can be seen that by increasing the value of the base acceleration from $1\,m/s^2$ to $9.81\,m/s^2$, the maximum average output power remarkably increases and changes from 35.4 μW to 20 mW.

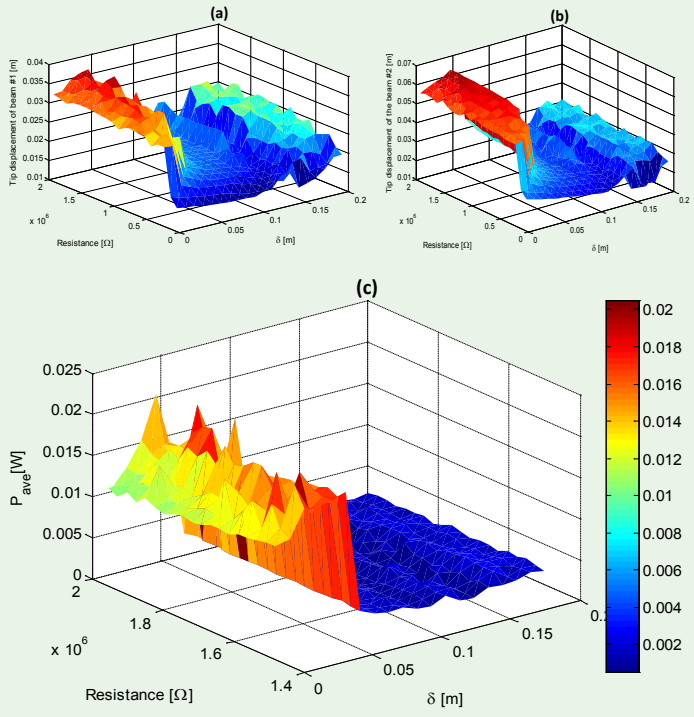

Figure 5: Influence of the clearance on **(a)** tip displacement of the beam #1, **(b)** tip displacement of the beam #2 and **(c)** the maximum average output power, for the coupling constant $k=400\,N/m$.

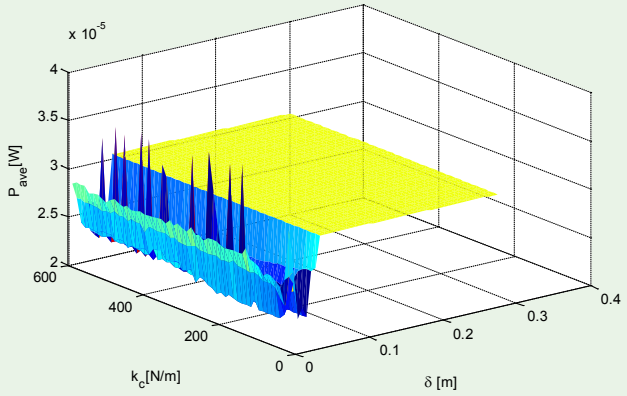

Figure 6: Influence of the clearance and coupling constant on the maximum average output power.

Figure 7 shows the influence of the piezoelectric layers length on output power while the excitation frequency ω_e is varying, for system parameters δ=15 mm, $k_c = 10^3\ N/m$, and the base acceleration of1g where g=9.81 m/s^2 , and external resistance load of $R_L = 1M\Omega$. In addition, the mechanical damping ratio ξ is considered to be equal to 0.5%.Also, in Figure (7a) and (7b) the length of the piezoelectric patches #1 and #2 are considered to be $L_{P_1} = 100mm$ and $L_{P_2} = 150mm$, respectively. It is seen that, the maximum output power for both Figure (6a) and (6b) occurs for $\omega_e = 3.034Hz$ which is close to primary resonance frequency of the thick beam. The value of the maximum average output power is equal to19 mW and 37 mW and occurs at $L_{P_1} = 76mm$ and $L_{P_2} = 66mm$, respectively. Figure (7c) shows the influence of the piezoelectric layers length on output power, while varying simultaneously, where considering the excitation frequency of the system is equal to the resonance frequency of the thick beam $\omega_e = \omega_{thick} = 3.08Hz$. As it is seen the value of the maximum output power is equal to 34 mW and occurs for the piezoelectric lengths of $L_{P_1} = 70mm$ and $L_{P_2} = 136mm$. It is worthy to note that in the following $L_{P_1} = 70mm$, $L_{P_2} = 136\ mm$ $L_{P_2} = 136mm$, and $R_L = 1M\Omega$ are used as values of the length of the piezoelectric patch #1 and the length of the piezoelectric patch #2, and the external resistance load, respectively.

Figure 8 shows the tip displacements and maximum average output power of the piezoelectric cantilever beams for three different coupling spring constants of 400 N/m, 800 N/m, and10^3N/m,and for the clearance of δ=15 mm, while varying the excitation frequency near the primary resonance frequency of the thick beam. It is seen that frequency response curves are tilted to the right, which represents a hardening behaviour. Corresponding to the specific values of the excitation frequency, there exist two stable solutions and for some values of the excitation frequency there appears one unstable solution, and below a critical value of excitation frequency there just exists one stable solution in the system. Furthermore, bifurcation can occur in the system due to the existence of the stable and unstable manifolds in the frequency response curves of the system. As it can be seen, for instance for the value of the coupling spring constant of, k=800 N/m,

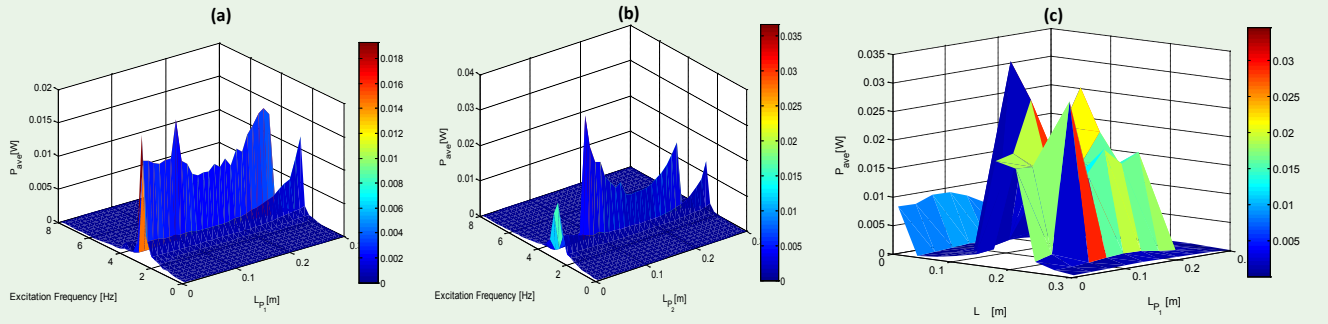

Figure 7: Influence of **(a)** length of the piezoelectric #1, and **(b)** length of the piezoelectric #2 on output power with respect to excitation frequency, and **(c)** influence of the piezoelectric layers length on maximum average output power for excitation frequency of, and the system parameters of $\delta = 15mm$, $k_c = 10^3\ N/m$, and base acceleration of $10\ m/s^2$.

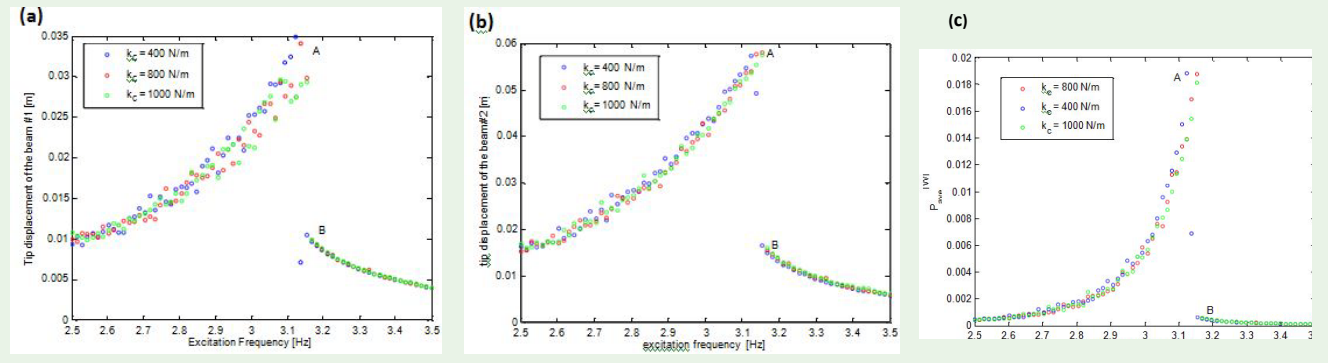

Figure 8: (a) Tip displacement of the beam #1, and **(b)** Tip displacement of the beam #2, and **(c)** maximum average output power, for three different values of the coupling spring constants $400\ N/m$, $800\ N/m$ and, $10^3\ N/m$ and clearance $\delta = 15mm$.

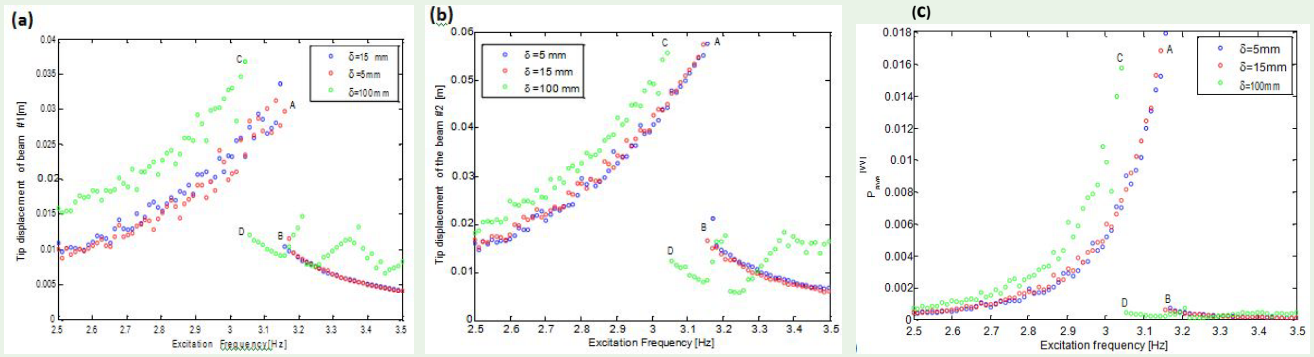

Figure 9: (a) Tip displacement of the beam #1, and **(b)** Tip displacement of the beam #2, and **(c)** maximum average output power, for three different values of the clearance,5 mm,15 mm and 100 mm, and for a fixed $k = 10^3 \, N/m$.

the stable branches meet the unstable one at fold bifurcation points A,B, for which depending on the initial conditions, the response may lay on either the stable or unstable branches. In addition, forward and backward frequency sweeps result in jumps and hysteresis phenomena in the response. For instance, for value of the coupling constant as k=800 N⁄m, a forward sweep passing point A results in a jump to the lower stable branch, and a backward sweep passing point B results in a jump to upper stable branch. As it is seen, the maximum stable amplitude for three different values of the coupling spring constant is close to each other, and the maximum average output power is less sensitive for value of the coupling constant, and increasing the value of the coupling spring constant does not affect the locus of the bifurcation points.

Figure 9 depicts tip displacements of the beams and maximum average output power versus excitation frequency for three different clearance of 5 mm,15 mm, and100 mm, and the coupling spring constant fixed at k=10³N⁄m, while varying the excitation frequency near the primary resonance frequency of the thick beam. It can be seen that the nonlinearity shifts the frequency response curves away from the frequency that can be predicted by a linear model, and frequency response curves are titled to the right, which represents a hardening behaviour. Nonlinear resonance frequency for three different values of the clearance between beams, 5 mm, 15 mm, and100 mm, occurs at 3.158 Hz, 3.148 Hz, and 3.044 Hz, respectively, and the corresponding maximum average output powers are equal to, 18 mW,16.8 mW, and 15.7 mW, respectively. As it is seen reducing the value of the clearance increases the possibility of impact between the beams, and it results in increasing the maximum average output power. It can be observed that increasing the value of the clearance alters the locus of bifurcation points and hysteresis region, and shifts the locus of the bifurcation points to the left.

Figure 10 depicts the influence of the external resistance load on maximum average output power for three different systems. Figure (10a) shows two types of systems i.e. a system by considering two beams in which the clearance between beams is considered to be δ=500 mm which as discussed in Figure 3 for this value of the clearance, the beams do not have contact with each other and they behave independently, and finally by considering that the system has only a single beam. Figure (10b) shows a system that consists of two coupled impacting beams. The maximum average output power is plotted with respect to external resistance load for two different values of the clearance between beams. To ensure that the beams are

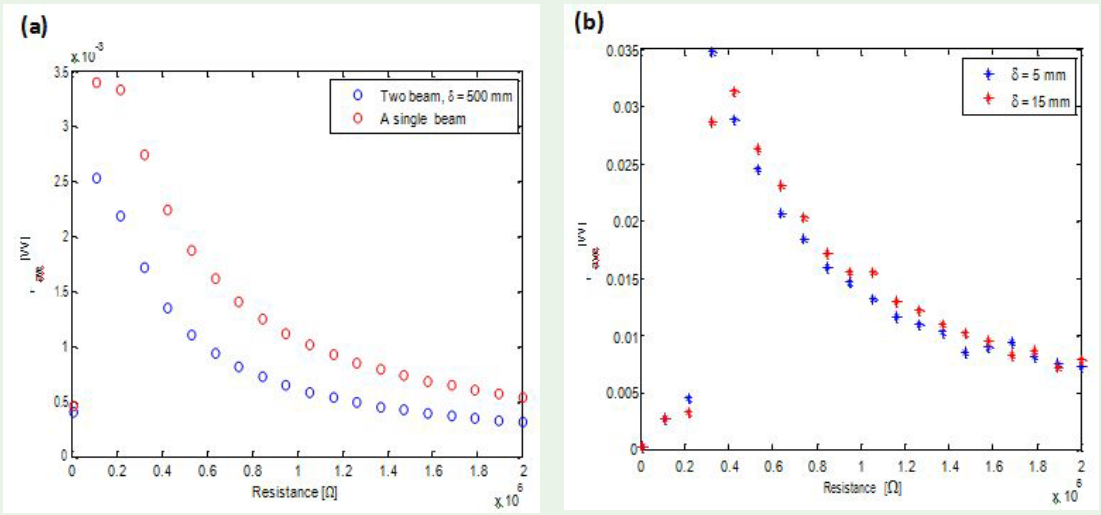

Figure 10: Influence of the external resistance load on **(a)** two beam with $\delta = 500mm$ and a single beam, and **(b)** two impacting beams for two different values of the clearance $\delta = 5mm$ and $\delta = 15mm$.

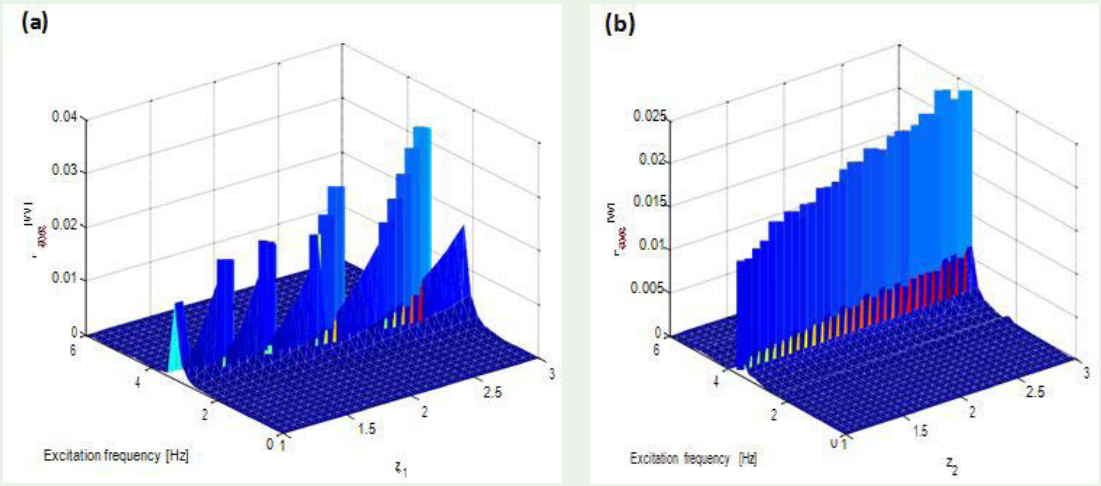

Figure 11: Influence of the **(a)** thickness ratio of the beams, and **(b)** thickness ratio of the piezoelectric layers on maximum average output power for coupling spring constant and clearance between beams fixed at $k = 10^3 \, N/m$, and $\delta = 15mm$ respectively.

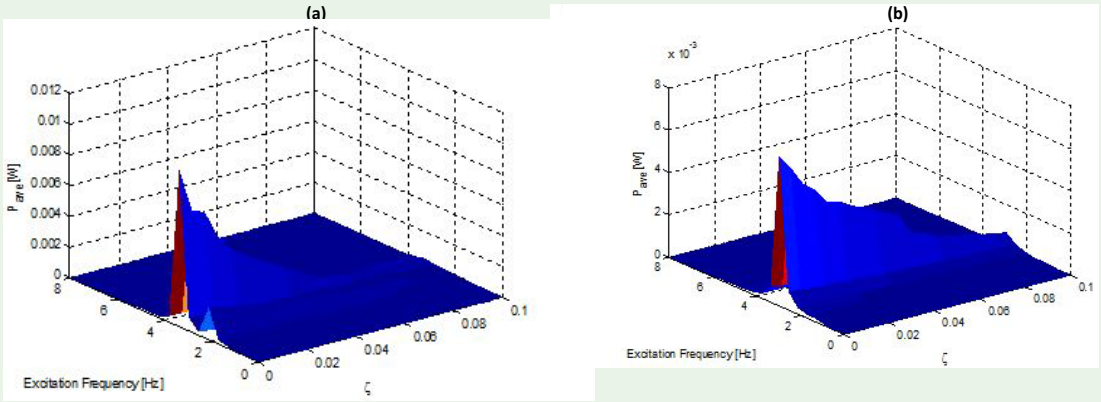

Figure 12: Variations of the maximum average output power with respect to excitation frequency for a system consisting of two beams **(a)** $\delta = 500mm$, and **(b)** $\delta = 15mm$.

in contact, the clearances between beams is considered to be δ=5 mm and δ=15mm. It can be observed that the maximum average output power is equal to 2.5 mW and 3.4 mW for the two beams, with δ=500 mm for a single beam, respectively, and the external resistance load in which the maximum average output power occurs is equal to 1.147 MΩ. It is seen that the maximum average output power for a system that has a single beam is more than a system that is consisted of two beams with no contact. It follows from the figure that the influence of the impact between beams is significant. As it is seen, the maximum average output power is equal to 34.67 mW and 31.26 mW for two different values of the clearance of δ=5 mm and δ=15mm, respectively, and occurs at the external resistance value of the 0.3 MΩ and 0.4 MΩ, respectively. As it is seen, the low value of the clearance and occurring impact in the system remarkably increases the value of the maximum average output power. In addition, the external resistance load where the maximum average output power happens is shifted to the left.

Figure 11 illustrates the influence of the thickness ratio of the beams and piezoelectric layers on the scavenged power. The coupling spring constant and clearance between beams are fixed at k=10^{3}N/m, and δ=15 mm respectively. In this figure z_1, and z_2 are defined as thickness ratio of the beams and piezoelectric layers, respectively. This study is carried out for the thickness of one beam and one piezoelectric patch fixed at 0.25 mm and 0.2 mm, respectively. Figure (11a) and (11b) are plotted for z_2=1.5 and z_1=2.73, respectively. As it is seen the maximum average output power is equal to 36 mW and 24 mW and occurs at z_1=2.73 and z_2=2.79, respectively, and the corresponding excitation frequencies in which the maximum average output occurs are 2.48 Hz and 3.72 Hz, which are close to primary resonance frequency of the thick beam for each system.

Figure 12 investigates the effect of the mechanical damping ratio on average output power with respect to excitation frequency for two types of systems i.e. a system consisting of two beams that the clearance between them is δ=500 mm for which the impact does not happen between the beams, and the other system that the clearance between beams is δ=15 mm for which the impact happens between beams where the coupling spring constant fixed at k=10^{3}N/m. It is seen that the maximum average output power occurs at ξ=0 for each case. It turns out that neglecting the mechanical damping ratio in the analysis of the energy harvester systems yields incorrect results.

Conclusions

In this paper, energy harvesting from large amplitude vibrations of a system consisting of two coupled impacting unimorph piezoelectric cantilever beams, for which it is assumed the whole system is subjected to a harmonic base excitation, was studied by considering nonlinearities in curvature. The mass and the gravitational potential of the piezoelectric layers, and cantilever beams were considered for the sake of completeness. The coupled governing equations of motion were derived using the Euler-Lagrange equations. The reduced-order model equations (ROMs) were obtained based on the Galerkin method. A parametric study on the tip displacements of the beams was carried out using a sine sweep across a frequency range, while the external resistance load is varying simultaneously. It was observed that the maximum amplitude for each of the beams occurs at the excitation frequency of $\omega_e = 3.01Hz$ which is near to primary resonance frequency of the thick beam. The effect of the different parameters such as clearance between beams, coupling spring constant, external resistance load, piezoelectric layers length, thickness ratio of the beams and piezoelectric layers, and the mechanical damping ratio were investigated on the scavenged power. It has been found that energy harvesting using impact significantly increases the output power. It was demonstrated that the power generated is highly sensitive to the clearance and the thickness ratio of the beams and piezoelectric layers, and is less sensitive to coupling spring constant. The effect of the clearance between beams was investigated and it was shown that high clearance between beams reduces the possibility of the impact, and hence reduces the value of the maximum average output power. In addition, the effect of the coupling spring constant was investigated and it has been demonstrated that the scavenged power is less sensitive to the coupling spring constant. The effect of the resistance load on scavenged power for three types of systems i.e. a system consisting of two beams with high clearance between beams in which the impact does not happen between beams, and a system consisting of two beams with low clearance in which impact happens between beams, and a system with a single beam was studied. It was observed that presence of the impact in the system remarkably increases the maximum average output power. The effect of the piezoelectric layers length on output power while the excitation frequency is varying was investigated and it was shown that the value of the maximum average output power is equal to, 19 mW, and 37 mW, and occurs at $L_{P_1} = 76mm$, and $L_{P_2} = 66mm$, respectively. Frequency response curves near the primary resonance were studied for different values of the clearance between beams and coupling spring constant. The effect of the clearance and coupling spring constant on the primary resonance was studied for the first mode. The results indicate that harvesting the maximum power output significantly depends on the proper choice of clearance and thickness ratio of the beams and piezoelectric layers and other parameters. The effect of the damping ratio on the output power while varying the excitation frequency, for two different values of the clearance, was studied and it was found that the presence of the damping ratio reduces the output power. The results of this study can be used to design novel nonlinear energy harvesters with large amplitude vibrations.

References

1. Remick K, Quinn DD, McFarland MD, Bergman L, Vakakis A. High-Frequency Vibration Energy Harvesting From Impulsive Excitation Utilizing Intentional Dynamic Instability Caused By Strong Nonlinearity. Journal of Sound and Vibration. 2016; 370: 259-279.
2. Jiang WA, Chen LQ. Stochastic Averaging Based on Generalized Harmonic Functions for Energy Harvesting Systems. Journal of Sound and Vibration. 2016; 377: 264-283.
3. Roundy S, Wright PK, Rabaey J. A Study of Low Level Vibrations as A Power Source for Wireless Sensor Nodes. Computer Communications. 2003; 26: 1131-1144.
4. Mitcheson PD, Green TC, Yeatman EM, Holmes AS. Architectures for Vibration-Driven Micropower Generators. Journal of Microelectromechanical Systems. 2004; 13: 429-440.
5. Leadenham S, Erturk A. M-Shaped Asymmetric Nonlinear Oscillator For Broadband Vibration Energy Harvesting: Harmonic Balance Analysis And Experimental Validation. Journal of Sound and Vibration. 2014; 333: 6209-6223.
6. Ahmadabadi ZN, Khadem SE. Nonlinear Vibration Control and Energy Harvesting of A Beam Using A Nonlinear Energy Sink and A Piezoelectric Device. Journal of Sound and Vibration. 2014; 333: 4444-4457.
7. Jiang WA, Chen LQ. Snap-Through Piezoelectric Energy Harvesting. Journal of Sound and Vibration. 2014; 333: 4314-4325.
8. Danesh-Yazdi AH, Elvin N, Andreopoulos Y. Green's Function Method for Piezoelectric Energy Harvesting Beams. Journal of Sound and Vibration. 2014; 333: 3092-3108.
9. Wang L, Yuan FG. Vibration Energy Harvesting By Magnetostrictive Material. Smart Materials and Structures. 2008; 17.
10. Adly A, Davino D, Giustiniani A, Visone C. Experimental Tests of A Magnetostrictive Energy Harvesting Device Toward its Modelling. Journal of Applied Physics. 2010; 107.
11. Erturk A, Inman DJ. Piezoelectric Energy Harvesting. John Wiley & Sons, 2011.
12. Beeby SP, Tudor MJ, White NM. Energy Harvesting Vibration Sources for Microsystems Applications. Measurement Science and Technology. 2006; 17.
13. Anton SR, Sodano HA. A Review of Power Harvesting Using Piezoelectric Materials (2003–2006). Smart materials and Structures. 2007; 16.
14. Kulah H, Najafi K. Energy Scavenging from Low-Frequency Vibrations by Using Frequency Up-Conversion for Wireless Sensor Applications. IEEE Sensors Journal. 2008; 8: 261-268.
15. Nguyen D, Halvorsen E, Jensen G, Vogl A. Fabrication and Characterization of A Wideband MEMS Energy Harvester Utilizing Nonlinear Springs. Journal of Micromechanics and Microengineering. 2010; 20.
16. Barton DA, Burrow SG, Clare LA. Energy harvesting from Vibrations with A Nonlinear Oscillator. Journal of Vibration and Acoustics. 2010; 132.
17. Ferrari M, Ferrari V, Guizzetti M, Andò B, Baglio S, Trigona C. Improved Energy Harvesting from Wideband Vibrations by Nonlinear Piezoelectric Converters. Sensors and Actuators A: Physical. 2010; 162: 425-431.
18. Harne RL, Wang KW. A review of the recent research on vibration energy harvesting via bistable systems. Smart Materials and Structures. 2013; 22.
19. Pellegrini SP, Tolou N, Schenk M, Herder JL. Bistable Vibration Energy Harvesters: A Review. Journal of Intelligent Material Systems and Structures. 2012; 24: 1303-1312.
20. Jiang S, Hu Y. Analysis of A Piezoelectric Bimorph Plate with A Central-Attached Mass as an Energy Harvester. IEEE transactions on Ultrasonics, Ferroelectrics, and Frequency Control. 2007; 54: 1463-1469.
21. Hu Y, Xue H, Hu H. A Piezoelectric Power Harvester with Adjustable Frequency Through Axial Preloads. Smart Materials and Structures. 2007; 16.
22. Hu HP, Cui ZJ, Cao JG. Performance of a piezoelectric bimorph harvester with variable width. Journal of Mechanics. 2007; 23: 197-202.

23. Erturk A, Inman DJ. A Distributed Parameter Electromechanical Model for Cantilevered Piezoelectric Energy Harvesters. Journal of Vibration and Acoustics. 2008; 130.

24. Panyam M, Masana R, Daqaq MF. On Approximating the Effective Bandwidth of Bi-Stable Energy Harvesters. International Journal of Non-Linear Mechanics. 2014; 67: 153-163.

25. Soliman MSM, Abdel-Rahman EM, El-Saadany EF, Mansour RR. A Wideband Vibration-Based Energy Harvester. Journal of Micromechanics and Microengineering.2008; 18.

26. Blystad LCJ, Halvorsen E, Husa S. Piezoelectric MEMS Energy Harvesting Systems Driven by Harmonic and Random Vibrations. IEEE Transactions on Ultrasonics Ferroelectrics and Frequency Control. 2010; 57: 908-919.

27. Blystad LCJ, Halvorsen E. A piezoelectric energy harvester with a mechanical end stop on one side. Microsystem Technologies. 2011; 17: 505-511.

28. Umeda M, Nakamura K, Ueha S. Analysis of the Transformation of Mechanical Impact Energy to Electric Energy Using Piezoelectric Vibrator. Japanese Journal of Applied Physics. 1996; 35.

29. Renaud M, Fiorini P, Van Hoof C. Optimization Of A Piezoelectric Unimorph For Shock And Impact Energy Harvesting. Smart Materials and Structures, 2007; 16.

30. Jacquelin E, Adhikari S, Friswell MI. A Piezoelectric Device for Impact Energy Harvesting. Smart Materials and Structures. 2011; 20.

31. Haroun A, Yamada I, Warisawa S. Study of Electromagnetic Vibration Energy Harvesting with Free/Impact Motion for Low Frequency Operation. Journal of Sound and Vibration. 2015; 349: 389-402.

32. Vijayan K, Friswell M, Khodaparast HH, Adhikari S. Non-Linear Energy Harvesting From Coupled Impacting Beams. International Journal of Mechanical Sciences. 2015; 97: 101-109.

33. Firoozy P, Khadem SE, Pourkiaee SM. Power Enhancement of Broadband Piezoelectric Energy Harvesting Using A Proof Mass And Nonlinearities In Curvature and Inertia. International Journal of Mechanical Sciences. 2017; 133: 227-239.

34. Firoozy P, Khadem SE, Pourkiaee SM. Broadband energy harvesting using nonlinear vibrations of a magnetopiezoelastic cantilever beam. International Journal of Engineering Science. 2017; 111: 113-133.

35. Rezaei M, Khadem SE, Firoozy P. Broadband and tunable PZT energy harvesting utilizing local nonlinearity and tip mass effects. International Journal of Engineering Science. 2017; 118: 1-15.

36. Wu GY. Non-linear vibration of bimaterial magneto-elastic cantilever beam with thermal loading. International Journal of Non-Linear Mechanics. 2013; 55: 10-18.